Outage Analysis of OFDM-Based Cognitive AF Relay Network in the Presence of Narrowband Interference

Samikkannu Rajkumar, V.N. Senthilkumaran, and S.J.Thiruvengadam

Orthogonal frequency-division multiplexing (OFDM) is one of the most widely used technologies in current wireless communication systems and standards. Cognitive radio (CR) provides a robust solution to the problem of spectrum congestion as it offers opportunistic usage of frequency bands that are not occupied by primary users. Due to the underlying sensing, spectrum shaping, scaling, and interoperable capabilities of OFDM, it has been adapted as a best transmission technology for CR wireless systems. However, the performance of an OFDM-based CR wireless system is affected by the existence of narrowband interference (NBI) from other users. Further, due to carrier frequency offset in NBI sources, NBI energy may spread over all subcarriers of an OFDM signal. In this paper, a fixed Amplify-and-Forward (AF) relay that operates at a frequency band that is different from that of direct mode is introduced to suppress the effect of NBI. Analytical expressions are derived for outage probability in direct, AF-relay, and incremental relaying modes. The outage performance of the proposed AF relay–based CR network is proven to be better than that of direct mode.

Keywords: Cognitive radio, AF relay, OFDM, CFO, NBI.

Manuscript received Mar. 10, 2014; revised Dec. 10, 2014; accepted Feb. 3, 2015.

Samikkannu Rajkumar (corresponding author, ssraj.tce@gmail.com), V.N. Senthilkumaran (vnsenthilkumaran@tce.edu), and S.J. Thiruvengadam (sjtece@tce.edu) are with the Department of Electronics and Communication Engineering, Thiagarajar College of Engineering, Tamil Nadu, India.

I. Introduction

Cognitive radio (CR) uses the available radio spectrum opportunistically to cope with the growing number of bandwidth-limited wireless services [1]. In a CR network, secondary users effectively utilize the unused spectrums of the primary users. Orthogonal frequency-division multiplexing (OFDM) is employed in a CR system due to its inherent characteristics of spectrum sensing, spectrum shaping, scaling, and interoperable capabilities [2]. Further, OFDM reduces fading caused by multiple receptions of a signal and hence improves spectral efficiency.

However, the performance of an OFDM-based CR system is affected by narrowband interference (NBI) from other wireless users. The following interference cancellation techniques are widely used in wireless communication systems: filter-based approach, cyclostationarity-based approach, higher-order statistics–based approach, transform domain approach, joint detection/multiuser detection (MUD), and spatial processing (for example, beamforming) [3]. Filter-based approaches were used to suppress NBI in OFDM-based conventional CR networks in [4]–[6]. In a coded OFDM system, NBI is suppressed by whitening the NBI spectrum using a prediction-error filter [4]. In [5], an interfering carrier frequency is estimated and cancelled using a notch filter. The success of this is dependent upon the accuracy of the estimation of the interfering carrier frequency. In [6], the active interfering tones in a multiband OFDM CR network are turned off and the resultant inter-carrier interference is suppressed using a notch filter. A higher-order statistics–based Bayesian decision

http://dx.doi.org/10.4218/etrij.15.0114.0300

theoretic approach is used to suppress partial-band interference in a frequency hop communication system [7]. However, this cannot be directly extended to an OFDM-based high-data-rate communication system due to its computational complexity. In [8], NBI is estimated by measuring the output signal energy, and receiver windowing is proposed to reduce the effect of NBI in an OFDM system.

In [9], using a linear minimum mean square error–based estimator, unmodulated subcarriers are employed to measure NBI power. As the energy of NBI is different at each subcarrier, it is considered as a colored noise, which is then compensated for using an iterative decoder based on an expectation–maximization algorithm [10]. A constrained minimum mean-output-energy–based algorithm is developed for NBI estimation under the assumption that the second-order statistics of a received signal are known at the receiver [11]. The major issue with this method is its high computational complexity. Compressive sensing is used to estimate an NBI signal by exploiting its sparsity in the frequency domain [12]. The effects of NBI are analyzed in an ultra-wideband cooperative relay network in [13].

Joint detection and MUD-based approaches were used for detecting secondary user symbols in the presence of a primary user signal, at the cost of high complexity [14]. In [15] and [16], interference is minimized in a CR system using the methods of opportunistic interference cancellation and phase adjustment, respectively. Amplify-and-Forward (AF) and Decode-and-Forward (DF) relaying protocols are used in cooperative communication networks to improve throughput and quality of service by exploiting spatial diversity [17]. The success of such a spatial processing technique has inspired us to use a co-operative AF half-duplex relay for interference cancellation. In this paper, the first major contribution is the introduction of a half-duplex AF relaying protocol in an OFDM-based CR network to suppress NBI. The use of such a relaying protocol provides spatial diversity and maximizes the output signal-to-interference-plus-noise ratio (SINR) of the CR network at each subcarrier of the OFDM signal. The second major contribution of this work is the derivation of the analytical expressions for analyzing the outage performance of the proposed OFDM-based cognitive AF relay network in the presence of NBI.

The rest of the paper is organized as follows. A system model for an OFDM-based cognitive AF relay network is described in both the time domain and the frequency domain for direct and AF relay modes, in Section II. The analytical expressions are derived for the SINR of the direct and AF relay modes, in Section III. The outage performance of an OFDM-based CR network is analyzed for direct, AF-relay, and incremental relaying modes, in Section IV. Numerical results are presented in Section V, and concluding remarks are given in Section VI.

Notations. Time-domain and frequency-domain vectors and matrices are denoted by $\mathbf{a}^{TD}$, $\mathbf{a}^{FD}$ and $\mathbf{A}^{TD}$, $\mathbf{A}^{FD}$, respectively, and scalars are indicated by lowercase letters. An $N \times N$ discrete Fourier transform (DFT) matrix and an $N \times N$ identity matrix are denoted by $\mathbf{F}_N$ and $\mathbf{I}_N$, respectively. An all-zero matrix of size $m \times n$ is denoted by $0_{m\times n}$. The matrix complex conjugate transpose, complex conjugate, transpose, and inverse operations are denoted by $(\,)^H$, $(\,)^*$, $(\,)^T$, and $(\,)^{-1}$, respectively.

II. System Model

Consider the OFDM-based cognitive AF relay network with three secondary users shown in Fig. 1. Such a network can operate in two modes; namely, direct mode and AF relay mode. In direct mode, SU1 transmits data to SU3 in the first time slot. In AF relay mode, SU1 transmits data to SU2, which acts as a relay, during the first time slot. The signal at SU2 is amplified and forwarded to SU3 in the second time slot. The frequency bands FB1, FB2, and FB3, which are available for transmission/reception at each secondary user, are also indicated in Fig. 1. The received signals at SU2 in relay mode and SU3 in direct/relay modes are affected by NBI from other sources in the scenario. It is assumed that the first secondary user, SU1, has to transmit an OFDM signal to the third secondary user, SU3, through a frequency-selective fading channel. The OFDM signal has N subcarriers and uses v zero-padded guard subcarriers to suppress intersymbol interference [18].

1. Direct Mode

In direct mode, SU1 transmits the OFDM signal to SU3 using the band FB1. The $L_1 \times 1$ channel impulse response (CIR) vector between SU1 and SU3 is defined as $\mathbf{h}_{13} = [h_{13}(0), h_{13}(1), \ldots, h_{13}(L_1-1)]^T$. The $L_2 \times 1$ CIR vector of NBI source two at SU3 is defined as $\mathbf{h}_{b3} = [h_{b3}(0), h_{b3}(1), \ldots, h_{b3}(L_2-1)]^T$.

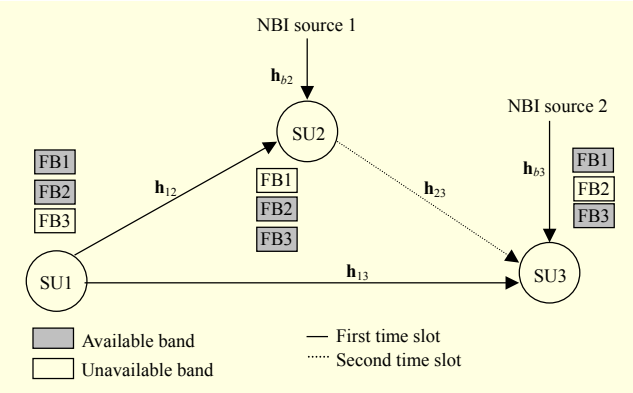

Fig. 1. AF relay–based CR network.

The $P \times 1$ time-domain received vector at SU3 is given by

$$\mathbf{y}_{13}^{\mathrm{TD}} = \mathbf{H}_{13}^{\mathrm{TD}} \mathbf{F}_{\mathrm{zp}} \mathbf{x}_1^{\mathrm{FD}} + \mathbf{A}_{\mathrm{fo},3}^{(1),\mathrm{TD}} \mathbf{H}_{b3}^{\mathrm{TD}} \mathbf{b}_3^{\mathrm{TD}} + \mathbf{z}_3^{\mathrm{TD}}, \quad (1)$$

where $P = N + v$; $\mathbf{H}_{13}^{\mathrm{TD}}$ and $\mathbf{H}_{b3}^{\mathrm{TD}}$ are $P \times P$ circulant matrices of an CIR vectors $\mathbf{h}_{13}$ and $\mathbf{h}_{b3}$, respectively; $\mathbf{F}_{\mathrm{zp}}$ is a $P \times N$ zero-padded inverse DFT matrix at SU1 (it is defined as $\mathbf{F}_{\mathrm{zp}} = \left[\mathbf{F}_N \, 0_{N \times v}\right]^{\mathrm{H}}$); $\mathbf{x}_1^{\mathrm{FD}}$ is a $N \times 1$ data vector at N subcarriers of an OFDM symbol; and $\mathbf{b}_3^{\mathrm{TD}}$ is a $P \times 1$ NBI signal vector at SU3. The interference power per subcarrier (IPPS) of an NBI signal is denoted by σ_{b3}^2; $\mathbf{z}_3^{\mathrm{TD}}$ is a $P \times 1$ zero-mean complex white Gaussian noise vector with elements that are independent and identically distributed with variance σ_{z3}^2. The carrier frequency offset (CFO) for an NBI signal in band FB1 is represented by a $P \times P$ diagonal matrix $\mathbf{A}_{\mathrm{fo},3}^{(1),\mathrm{TD}} = \mathrm{diag}\left\{1, \exp\left(\mathrm{j}2\pi\beta(1)/P\right), \ldots, \exp\left(\mathrm{j}2\pi\beta(P-1)/P\right)\right\}$, where β is a uniformly distributed random variable over the interval $\left[-1/2, 1/2\right]$ [19]. By taking a DFT, the frequency-domain representation of the received vector $\mathbf{y}_{13}^{\mathrm{TD}}$ in (1) is given by

$$\mathbf{y}_{13}^{\mathrm{FD}} = \mathbf{F}_p \mathbf{y}_{13}^{\mathrm{TD}} = \mathbf{F}_p \left(\mathbf{H}_{13}^{\mathrm{TD}} \mathbf{F}_{\mathrm{zp}} \mathbf{x}_1^{\mathrm{FD}} + \mathbf{A}_{\mathrm{fo},3}^{(1),\mathrm{TD}} \mathbf{H}_{b3}^{\mathrm{TD}} \mathbf{b}_3^{\mathrm{TD}} + \mathbf{z}_3^{\mathrm{TD}} \right). \quad (2)$$

Since $\mathbf{H}_{13}^{\mathrm{TD}}$ and $\mathbf{H}_{b3}^{\mathrm{TD}}$ are circulant matrices, they can be decomposed as $\mathbf{H}_{13}^{\mathrm{TD}} = \mathbf{F}_P^{\mathrm{H}} \mathbf{H}_{13}^{\mathrm{FD}} \mathbf{F}_P$ and $\mathbf{H}_{b3}^{\mathrm{TD}} = \mathbf{F}_P^{\mathrm{H}} \mathbf{H}_{b3}^{\mathrm{FD}} \mathbf{F}_P$ [20], where $\mathbf{H}_{13}^{\mathrm{FD}}$ and $\mathbf{H}_{b3}^{\mathrm{FD}}$ are diagonal matrices. Let $\boldsymbol{\lambda}_{13} = \left[\lambda_{13}(0), \lambda_{13}(1), \ldots, \lambda_{13}(P-1)\right]^{\mathrm{T}}$ and $\boldsymbol{\lambda}_{b3} = \left[\lambda_{b3}(0), \lambda_{b3}(1), \ldots, \lambda_{b3}(P-1)\right]^{\mathrm{T}}$ be P-point DFTs of $\mathbf{h}_{13}$ and $\mathbf{h}_{b3}$, respectively. Then, the matrices $\mathbf{H}_{13}^{\mathrm{FD}}$ and $\mathbf{H}_{b3}^{\mathrm{FD}}$ are defined as $\mathbf{H}_{13}^{\mathrm{FD}} = \mathrm{diag}\left\{\lambda_{13}(0), \lambda_{13}(1), \ldots, \lambda_{13}(P-1)\right\}$ and $\mathbf{H}_{b3}^{\mathrm{FD}} = \mathrm{diag}\left\{\lambda_{b3}(0), \lambda_{b3}(1), \ldots, \lambda_{b3}(P-1)\right\}$. Now, (2) can be simply written as

$$\mathbf{y}_{13}^{\mathrm{FD}} = \mathbf{H}_{13}^{\mathrm{FD}} \mathbf{V} \mathbf{x}_1^{\mathrm{FD}} + \mathbf{A}_3^{(1),\mathrm{FD}} \mathbf{H}_{b3}^{\mathrm{FD}} \mathbf{b}_3^{\mathrm{FD}} + \mathbf{z}_3^{\mathrm{FD}}, \quad (3)$$

where $\mathbf{V} = \mathbf{F}_P \mathbf{F}_{\mathrm{zp}}$ is the precoding matrix; $\mathbf{A}_3^{(1),\mathrm{FD}} = \mathbf{F}_P \mathbf{A}_3^{(1),\mathrm{TD}} \mathbf{F}_P^{\mathrm{H}}$ is a circulant matrix of CFO at SU3; and $\mathbf{b}_3^{\mathrm{FD}}$ and $\mathbf{z}_3^{\mathrm{FD}}$ are the NBI signal and noise vectors in the frequency domain, respectively. The $P \times 1$ NBI signal vector the vector $\mathbf{b}_3^{\mathrm{FD}}$ is sparse in nature and indicates that $\mathbf{b}_3^{\mathrm{FD}}$ contains only a few non-zero elements. The kth subcarrier element $b_3(k) \neq 0$ if $k \in I_{b3}$, where I_{b3} is a set that contains an index of the non-zero elements which is NBI affected subcarriers.

2. AF Relay Mode

In AF relay mode, SU1 transmits an OFDM signal to SU2 using the band FB2 in the first time slot. The $L_3 \times 1$ CIR vector between SU1 and SU2 is defined as $\mathbf{h}_{12} = \left[h_{12}(0), h_{12}(1), \ldots, h_{12}(L_3 - 1)\right]^{\mathrm{T}}$. The $L_4 \times 1$ CIR vector between NBI source one and SU2 is defined as $\mathbf{h}_{b2} = \left[h_{b2}(0), h_{b2}(1), \ldots, h_{b2}(L_4 - 1)\right]^{\mathrm{T}}$. The $P \times 1$ time-domain received vector $\mathbf{y}_{12}^{\mathrm{TD}}$ at SU2 is given by

$$\mathbf{y}_{12}^{\mathrm{TD}} = \mathbf{H}_{12}^{\mathrm{TD}} \mathbf{F}_{\mathrm{zp}} \mathbf{x}_1^{\mathrm{FD}} + \mathbf{A}_{\mathrm{fo},2}^{(2),\mathrm{TD}} \mathbf{H}_{b2}^{\mathrm{TD}} \mathbf{b}_2^{\mathrm{TD}} + \mathbf{z}_2^{\mathrm{TD}}, \quad (4)$$

where $\mathbf{H}_{12}^{\mathrm{TD}}$ and $\mathbf{H}_{b2}^{\mathrm{TD}}$ are the $P \times P$ circulant matrices of the CIR vectors $\mathbf{h}_{12}$ and $\mathbf{h}_{b2}$, respectively. In addition, $\mathbf{b}_2^{\mathrm{TD}}$ and $\mathbf{z}_2^{\mathrm{TD}}$ are the NBI signal and noise vectors at SU2, respectively, and $\mathbf{A}_{\mathrm{fo},2}^{(2),\mathrm{TD}}$ is the CFO of the NBI signal in band FB2. By taking a DFT, the frequency-domain representation of the received vector $\mathbf{y}_{12}^{\mathrm{TD}}$ is given by

$$\mathbf{y}_{12}^{\mathrm{FD}} = \mathbf{F}_p \mathbf{y}_{12}^{\mathrm{TD}} = \mathbf{F}_p \left(\mathbf{H}_{12}^{\mathrm{TD}} \mathbf{F}_{\mathrm{zp}} \mathbf{x}_1^{\mathrm{FD}} + \mathbf{A}_{\mathrm{fo},2}^{(2),\mathrm{TD}} \mathbf{H}_{b2}^{\mathrm{TD}} \mathbf{b}_2^{\mathrm{TD}} + \mathbf{z}_2^{\mathrm{TD}} \right). \quad (5)$$

Since $\mathbf{H}_{12}^{\mathrm{TD}}$ and $\mathbf{H}_{b2}^{\mathrm{TD}}$ are circulant matrices, (5) can be simplified as

$$\mathbf{y}_{12}^{\mathrm{FD}} = \mathbf{H}_{12}^{\mathrm{FD}} \mathbf{V} \mathbf{x}_1^{\mathrm{FD}} + \mathbf{A}_2^{(2),\mathrm{FD}} \mathbf{H}_{b2}^{\mathrm{FD}} \mathbf{b}_2^{\mathrm{FD}} + \mathbf{z}_2^{\mathrm{FD}}, \quad (6)$$

where $\mathbf{H}_{12}^{\mathrm{FD}}$ and $\mathbf{H}_{b2}^{\mathrm{FD}}$ are the diagonal matrices of the vectors $\boldsymbol{\lambda}_{12}$ and $\boldsymbol{\lambda}_{b2}$, respectively, and $\mathbf{A}_2^{(2),\mathrm{FD}} = \mathbf{F}_P \mathbf{A}_2^{(2),\mathrm{TD}} \mathbf{F}_P^{\mathrm{H}}$ is a circulant matrix.

In the second time slot, the node of SU2 plays as an AF relay. It amplifies the received signal $\mathbf{y}_{12}^{\mathrm{TD}}$ and forwards it to SU3 using the band FB3. The $L_5 \times 1$ CIR vector between SU2 and SU3 is defined as $\mathbf{h}_{23} = \left[h_{23}(0), h_{23}(1), \ldots, h_{23}(L_5 - 1)\right]^{\mathrm{T}}$. The $L_6 \times 1$ CIR vector of NBI source two at SU3 is defined as $\mathbf{h}_{b3} = \left[h_{b3}(0), h_{b3}(1), \ldots, h_{b3}(L_6 - 1)\right]$. The time-domain received vector $\mathbf{y}_{23}^{\mathrm{TD}}$ at SU3 is given by

$$\mathbf{y}_{23}^{\mathrm{TD}} = \rho \mathbf{H}_{23}^{\mathrm{TD}} \left(\mathbf{y}_{12}^{\mathrm{TD}} \right) + \mathbf{A}_{\mathrm{fo},3}^{(3),\mathrm{TD}} \mathbf{H}_{b3}^{\mathrm{TD}} \mathbf{b}_3^{\mathrm{TD}} + \mathbf{n}_3^{\mathrm{TD}}, \quad (7)$$

where $\rho = \sqrt{\mathrm{P}_s \Big/ \left(\mathrm{P}_s \sigma_h^2 + \sigma_{b2}^2 + \sigma_{z2}^2 \right)}$ is the amplification factor at SU2; $\sigma_h^2 = \mathrm{E}\left[\left| \mathbf{h}_{12} \right|^2 \right]$ is the instantaneous squared-norm of the CIR vector $\mathbf{h}_{12}$; $\mathrm{P}_s = \mathrm{E}\left[\left| \mathbf{x}_1^{\mathrm{FD}} \right|^2 \right]$ is the transmitted source power, which is the same as in SU2; σ_{b2}^2 is the IPPS of the NBI signal vector $\mathbf{b}_2^{\mathrm{TD}}$; σ_{z2}^2 is the variance of the noise vector $\mathbf{z}_2^{\mathrm{TD}}$; and $\mathbf{H}_{23}^{\mathrm{TD}}$ and $\mathbf{H}_{b3}^{\mathrm{TD}}$ are the circulant matrices of the CIR vectors $\mathbf{h}_{23}$ and $\mathbf{h}_{b3}$, respectively. In addition, $\mathbf{A}_{\mathrm{fo},3}^{(3),\mathrm{TD}}$, $\mathbf{b}_3^{\mathrm{TD}}$, and $\mathbf{n}_3^{\mathrm{TD}}$ represent the CFO for NBI in band FB3 and the NBI signal and noise vectors at SU3, respectively. Substituting (4) in (7), the received vector $\mathbf{y}_{23}^{\mathrm{TD}}$ is written as

$$\begin{aligned} \mathbf{y}_{23}^{\mathrm{TD}} = {} & \rho \mathbf{H}_{23}^{\mathrm{TD}} \mathbf{H}_{12}^{\mathrm{TD}} \mathbf{F}_{\mathrm{zp}} \mathbf{x}_1^{\mathrm{FD}} + \rho \mathbf{H}_{23}^{\mathrm{TD}} \mathbf{A}_{\mathrm{fo},2}^{(2),\mathrm{TD}} \mathbf{H}_{b2}^{\mathrm{TD}} \mathbf{b}_2^{\mathrm{TD}} \\ & + \mathbf{A}_{\mathrm{fo},3}^{(3),\mathrm{TD}} \mathbf{H}_{b3}^{\mathrm{TD}} \mathbf{b}_3^{\mathrm{TD}} + \rho \mathbf{H}_{23}^{\mathrm{TD}} \mathbf{z}_2^{\mathrm{TD}} + \mathbf{n}_3^{\mathrm{TD}}. \end{aligned} \quad (8)$$

By taking a DFT, the frequency-domain representation of the received vector $\mathbf{y}_{23}^{\mathrm{TD}}$ is given by

$$\mathbf{y}_{23}^{\mathrm{FD}} = \mathbf{F}_p \mathbf{y}_{23}^{\mathrm{TD}} = \mathbf{F}_p \left\{ \rho \mathbf{H}_{23}^{\mathrm{TD}} \mathbf{H}_{12}^{\mathrm{TD}} \mathbf{F}_{\mathrm{zp}} \mathbf{x}_1^{\mathrm{FD}} + \rho \mathbf{H}_{23}^{\mathrm{TD}} \mathbf{A}_{\mathrm{fo},2}^{(2),\mathrm{TD}} \mathbf{H}_{b2}^{\mathrm{TD}} \mathbf{b}_2^{\mathrm{TD}} + \mathbf{A}_{\mathrm{fo},3}^{(3),\mathrm{TD}} \mathbf{H}_{b3}^{\mathrm{TD}} \mathbf{b}_3^{\mathrm{TD}} + \rho \mathbf{H}_{23}^{\mathrm{TD}} \mathbf{z}_2^{\mathrm{TD}} + \mathbf{n}_3^{\mathrm{TD}} \right\}, \tag{9}$$

where $\mathbf{H}_{23}^{\mathrm{TD}}, \mathbf{H}_{12}^{\mathrm{TD}}, \mathbf{H}_{b2}^{\mathrm{TD}}$, and $\mathbf{H}_{b3}^{\mathrm{TD}}$ are circulant matrices. By decomposing them, (9) can be simplified as

$$\mathbf{y}_{23}^{\mathrm{FD}} = \rho \mathbf{H}_{23}^{\mathrm{FD}} \mathbf{H}_{12}^{\mathrm{FD}} \mathbf{V} \mathbf{x}_1^{\mathrm{FD}} + \rho \mathbf{H}_{23}^{\mathrm{FD}} \mathbf{A}_2^{(2),\mathrm{FD}} \mathbf{H}_{b2}^{\mathrm{FD}} \mathbf{b}_2^{\mathrm{FD}} + \mathbf{A}_3^{(3),\mathrm{FD}} \mathbf{H}_{b3}^{\mathrm{FD}} \mathbf{b}_3^{\mathrm{FD}} + \rho \mathbf{H}_{23}^{\mathrm{FD}} \mathbf{z}_2^{\mathrm{FD}} + \mathbf{n}_3^{\mathrm{FD}}. \tag{10}$$

Let $\boldsymbol{\lambda}_{23} = \left[\lambda_{23}(0), \lambda_{23}(1), \ldots, \lambda_{23}(P-1)\right]^{\mathrm{T}}$ and $\boldsymbol{\lambda}_{b3} = \left[\lambda_{b3}(0), \lambda_{b3}(1), \ldots, \lambda_{b3}(P-1)\right]^{\mathrm{T}}$ be P-point DFTs of $\mathbf{h}_{23}$ and $\mathbf{h}_{b3}$, respectively. The elements of the diagonal matrices $\mathbf{H}_{23}^{\mathrm{FD}}$ and $\mathbf{H}_{b3}^{\mathrm{FD}}$ are the vectors $\boldsymbol{\lambda}_{23}$ and $\boldsymbol{\lambda}_{b3}$, respectively; $\mathbf{A}_3^{(3),\mathrm{FD}} = \mathbf{F}_P \mathbf{A}_3^{(3),\mathrm{TD}} \mathbf{F}_P^{\mathrm{H}}$ is a circulant matrix.

III. SINR Analysis

In this section, the analytical expressions for the SINR of the received signals at relay and destination nodes are derived at each subcarrier in both direct and AF relay modes.

1. Direct Mode

From (3), the direct-mode receive signal $\mathbf{y}_{13}^{\mathrm{FD}}$ at the kth subcarrier is given by

$$y_{13}(k) = \lambda_{13}(k) v(k,k) x_1(k) + \lambda_{13}(k) \sum_{q=0, q\neq k}^{N-1} v(k,q) x_1(q) + \sum_{m=0, m\in I_{b3}}^{P-1} \lambda_{b3}(m) a_3^1\left(k, (m-k)_P\right) b_3(m) + z_3(k) \quad \text{for } k = 0,1,2,\ldots,P-1. \tag{11}$$

In this expression, the first term is the desired signal, where $x_1(k)$ is the kth subcarrier source data. The second and third terms denote the residual zero-padded interference and NBI signal, respectively. Since $\mathbf{A}_3^{(1),\mathrm{FD}}$ is a circulant matrix, the third term is written as a circular convolution. The fourth term represents the noise at the kth subcarrier.

Assuming that the CIR vectors $\boldsymbol{\lambda}_{13}$ and $\boldsymbol{\lambda}_{b3}$ are perfectly known, the instantaneous SINR of the direct-mode receive signal $\mathbf{y}_{13}^{\mathrm{FD}}$ at the kth subcarrier is given by

$$\Gamma_{13}(k) = \frac{\left|\lambda_{13}(k)\right|^2 \left|v(k,k)\right|^2 \mathrm{E}\left(\left|x_1(k)\right|^2\right)}{\left\{\left|\lambda_{13}(k)\right|^2 \mathrm{E}\left(\left|\sum_{q=0, q\neq k}^{N-1} v(k,q) x_1(q)\right|^2\right) + \mathrm{E}\left(\left|\sum_{m=0, m\in I_{b3}}^{P-1} \lambda_{b3}(m) a_3^1\left(k, (m-k)_P\right) b_3(m)\right|^2\right) + \mathrm{E}\left(\left|z_3(k)\right|^2\right)\right\}}. \tag{12}$$

Using the Cauchy–Schwartz inequality, the first term in the denominator of (12) can be expressed as

$$\mathrm{E}\left(\left|\sum_{q=0, q\neq k}^{N-1} v(k,q) x_1(q)\right|^2\right) \le \sum_{q=0, q\neq k}^{N-1} \left|v(k,q)\right|^2 \mathrm{E}\left(\sum_{q=0, q\neq k}^{N-1} \left|x_1(q)\right|^2\right). \tag{13}$$

Since $\sum_{q=0}^{N-1} \left|v(k,q)\right|^2 = 1$, the term $\sum_{q=0, q\neq k}^{N-1} \left|v(k,q)\right|^2$ can be simplified as $1 - \left|v(k,k)\right|^2$; then (13) can be written as

$$\mathrm{E}\left(\left|\sum_{q=0, q\neq k}^{N-1} v(k,q) x_1(q)\right|^2\right) \le \left(1 - \left|v(k,k)\right|^2\right) \mathrm{P_s}. \tag{14}$$

Similarly, the second term in the denominator of (12) can be expressed as

$$\mathrm{E}\left(\left|\sum_{m=0, m\in I_{b3}}^{P-1} \lambda_{b3}(m) a_3^1\left(k, (m-k)_P\right) b_3(m)\right|^2\right) \le \sum_{m=0, m\in I_{b3}}^{P-1} \left|\lambda_{b3}(m)\right|^2 \varsigma_3 \sigma_{b3}^2, \tag{15}$$

where $\varsigma_3 = \sum_{m=0, m\in I_{b3}}^{P-1} \left|a_3^1\left(k, (m-k)_P\right)\right|^2$ is the squared-norm of the CFO term and $\sigma_{b3}^2 = \mathrm{E}\left(\sum_{m=0, m\in I_{b3}}^{P-1} \left|b_3(m)\right|^2\right)$ is the IPPS of the NBI term. Now, substituting (14) and (15) in (12), the lower bound of $\Gamma_{13}(k)$ is simply written as

$$\Gamma_{13}(k) \ge \frac{\left|\lambda_{13}(k)\right|^2 \left|v(k,k)\right|^2 \mathrm{P_s}}{\left|\lambda_{13}(k)\right|^2 \left(1 - \left|v(k,k)\right|^2\right) \mathrm{P_s} + \sum_{m=0, m\in I_{b3}}^{P-1} \left|\lambda_{b3}(m)\right|^2 \varsigma_3 \sigma_{b3}^2 + \sigma_{z3}^2}, \tag{16}$$

where $\sigma_{z3}^2 = \mathrm{E}\left(\left|z_3(k)\right|^2\right)$ is the noise variance. Dividing the numerator and denominator by the source power $\mathrm{P_s}$, we get

$$\Gamma_{13}(k) \ge \frac{\left|\lambda_{13}(k)\right|^2 \left|v(k,k)\right|^2}{\left|\lambda_{13}(k)\right|^2 \left(1 - \left|v(k,k)\right|^2\right) + \sum_{m=0, m\in I_{b3}}^{P-1} \left|\lambda_{b3}(m)\right|^2 \varsigma_3 \frac{1}{\mathrm{SIR1}} + \frac{1}{\mathrm{SNR}}}, \tag{17}$$

where $\mathrm{SIR1} = \mathrm{P_s} / \sigma_{b3}^2$ and $\mathrm{SNR} = \mathrm{P_s} / \sigma_{z3}^2$.

2. AF Relay Mode

In AF relay mode, a transmit signal passes through the two different channels $\mathbf{h}_{12}$ and $\mathbf{h}_{23}$ with amplification factor ρ at SU2. The SINR between SU1 and SU3 at the kth subcarrier in AF relay mode, $\Gamma_{123}(k)$, is given by [21] as

$$\Gamma_{123}(k) = \left[\Gamma_{12}(k) \Gamma_{23}(k)\right] / \left[\Gamma_{12}(k) + \Gamma_{23}(k) + 1\right], \tag{18}$$

where $\Gamma_{IJ}(k)$ is the SINR of the link joining SUI and SUJ,

$I, J \in (1,2)$. The SINR of the link joining SU1 and SU2 is determined as follows. From (6), the received signal $\mathbf{y}_{12}^{\mathrm{FD}}$ from SU1 to SU2 at the kth subcarrier is given by

$$y_{12}(k) = \lambda_{12}(k)v(k,k)x_1(k) + \lambda_{12}(k)\sum_{q=0,q\neq k}^{N-1} v(k,q)x_1(q) + \sum_{m=0,m\in I_{b2}}^{P-1} \lambda_{b2}(m)a_2^2\left(k,(m-k)_P\right)b_2(m) + z_2(k), \quad k = 0,1,\ldots,P-1. \tag{19}$$

In this expression, the first term is the desired signal. The second and third terms denote the residual zero-padded interference and the NBI signal, respectively. The fourth term is the noise. The instantaneous SINR of the received signal $y_{12}(k)$ is given by

$$\Gamma_{12}(k) = \frac{\left|\lambda_{12}(k)\right|^2 \left|v(k,k)\right|^2 \mathrm{E}\left(\left|x_1(k)\right|^2\right)}{\left\{\left|\lambda_{12}(k)\right|^2 \mathrm{E}\left(\left|\sum_{q=0,q\neq k}^{N-1} v(k,q)x_1(q)\right|^2\right) + \mathrm{E}\left(\left|\sum_{m=0,m\in I_{b2}}^{P-1} \lambda_{b2}(m)a_2^2\left(k,(m-k)_P\right)b_2(m)\right|^2\right) + \mathrm{E}\left(\left|z_2(k)\right|^2\right)\right\}}. \tag{20}$$

The first and second terms in the denominator of (20) can be simplified as

$$\mathrm{E}\left(\left|\sum_{q=0,q\neq k}^{N-1} v(k,q)x_1(q)\right|^2\right) \le \left(1-\left|v(k,k)\right|^2\right)\mathrm{P_s} \tag{21}$$

and

$$\mathrm{E}\left(\left|\sum_{m=0,m\in I_{b2}}^{P-1} \lambda_{b2}(m)a_2^2\left(k,(m-k)_P\right)b_2(m)\right|^2\right) \le \sum_{m=0,m\in I_{b2}}^{P-1} \left|\lambda_{b2}(m)\right|^2 \varsigma_2\sigma_{b2}^2, \tag{22}$$

respectively, where $\varsigma_2 = \sum_{m=0,m\in I_{b2}}^{P-1} \left|a_2^2\left(k,(m-k)_P\right)\right|^2$ is the squared-norm of the CFO term and $\sigma_{b2}^2 = \left(\sum_{m=0,m\in I_{b2}}^{P-1} \left|b_2(m)\right|^2\right)$ is the IPPS of the NBI term. Substituting (21) and (22) in (20), we get

$$\Gamma_{12}(k) \ge \frac{\left|\lambda_{12}(k)\right|^2 \left|v(k,k)\right|^2}{\left|\lambda_{12}(k)\right|^2\left(1-\left|v(k,k)\right|^2\right) + \sum_{m=0,m\in I_{b2}}^{P-1} \left|\lambda_{b2}(m)\right|^2 \varsigma_2 \frac{1}{\mathrm{SIR2}} + \frac{1}{\mathrm{SNR}}}, \tag{23}$$

where $\mathrm{SIR2} = \mathrm{P_s}/\sigma_{b2}^2$, $\mathrm{SNR} = \mathrm{P_s}/\sigma_{z2}^2$, and σ_{z2}^2 is the noise variance. The instantaneous SINR of the received signal $\mathbf{y}_{23}^{\mathrm{FD}}$ can be expressed as

$$\Gamma_{23}(k) = \frac{\left|\lambda_{23}(k)\right|^2 \left|v(k,k)\right|^2 \mathrm{E}\left(\left|x_1(k)\right|^2\right)}{\left\{\left|\lambda_{23}(k)\right|^2 \mathrm{E}\left(\left|\sum_{q=0,q\neq k}^{N-1} v(k,q)x_1(q)\right|^2\right) + \mathrm{E}\left(\left|\sum_{m=0,m\in I_{b3}}^{P-1} \lambda_{b3}(m)a_3^3\left(k,(m-k)_P\right)b_3(m)\right|^2\right) + \mathrm{E}\left(\left|n_3(k)\right|^2\right)\right\}}. \tag{24}$$

The first and second terms in the denominator of (24) can be simplified as

$$\mathrm{E}\left(\left|\sum_{q=0,q\neq k}^{N-1} v(k,q)x_1(q)\right|^2\right) \le \left(1-\left|v(k,k)\right|^2\right)\mathrm{P_s} \tag{25}$$

and

$$\mathrm{E}\left(\left|\sum_{m=0,m\in I_{b3}}^{P-1} \lambda_{b3}(m)a_3^3\left(k,(m-k)_P\right)b_3(m)\right|^2\right) \le \sum_{m=0,m\in I_{b3}}^{P-1} \left|\lambda_{b3}(m)\right|^2 \varsigma_3''\sigma_{b3}^2, \tag{26}$$

respectively, where $\varsigma_3'' = \sum_{m=0,m\in I_{b3}}^{P-1} \left|a_3^3\left(k,(m-k)_P\right)\right|^2$ is the squared-norm of the CFO and $\sigma_{b3}^2 = \left(\sum_{m=0,m\in I_{b3}}^{P-1} \left|b_3(m)\right|^2\right)$ is the IPPS of the NBI term. Substituting (25) and (26) in (24), we get

$$\Gamma_{23}(k) \ge \frac{\left|\lambda_{23}(k,k)\right|^2 \left|v(k,k)\right|^2}{\left|\lambda_{23}(k,k)\right|^2\left(1-\left|v(k,k)\right|^2\right) + \sum_{m=0,m\in I_{b3}}^{P-1} \left|\lambda_{b3}(m)\right|^2 \varsigma_3'' \frac{1}{\mathrm{SIR3}} + \frac{1}{\mathrm{SNR}}}, \tag{27}$$

where $\mathrm{SIR3}=\mathrm{P_s}/\sigma_{b3}^2$, $\mathrm{SNR}=\mathrm{P_s}/\sigma_{n3}^2$, and $\sigma_{n3}^2=\mathrm{E}\left(\left|n_3(k)\right|^2\right)$ is the noise variance. In AF relay mode, the maximum data transfer rate depends on the minimum value between $\Gamma_{12}(k)$ and $\Gamma_{23}(k)$. Hence, the SINR $\Gamma_{123}(k)$ in AF mode is written as

$$\Gamma_{123}(k) = \frac{\Gamma_{12}(k)\Gamma_{23}(k)}{\Gamma_{12}(k)+\Gamma_{23}(k)+1} \le \min\left(\Gamma_{12}(k),\Gamma_{23}(k)\right). \tag{28}$$

IV. Performance Analysis

In this section, the outage performance of the OFDM-based cognitive AF relay network is analyzed at the subcarrier level in direct and AF relay modes for the data rate of R b/s/Hz. In addition, outage of the incremental AF relay is analyzed.

1. Outage Probability Analysis in Direct Mode

In direct mode, the upper bound of the outage probability of Γ_{13} at the kth subcarrier for the given data rate of R b/s/Hz is

defined as

$$P_{\text{out},k}^{\text{dir}}(R) \le P\left(\log_2\left(1+\Gamma_{13}(k)\right) < R\right). \quad (29)$$

Let the threshold SINR $\gamma_1 = 2^R - 1$. Then, the upper bound of $P_{\text{out},k}^{\text{dir}}(R)$ can be written as

$$P_{\text{out},k}^{\text{dir}}(R) \le P\left(\Gamma_{13}(k) < \gamma_1\right). \quad (30)$$

The probability density function (PDF) of $\Gamma_{13}(k)$ is determined as follows. Let (17) be defined as

$$\Gamma_{13}(k) = \frac{aX}{bY + cZ + d}, \quad (31)$$

where $X = Y = |\lambda_{13}(k)|^2$, $Z = \sum_{m=0, m\in I_{b3}}^{P-1} |\lambda_{b3}(m)|^2$, $a = |v(k,k)|^2$, $b = \left(1 - |v(k,k)|^2\right)$, $c = \varsigma_3\left(1/\text{SIR1}\right)$, and $d = 1/\text{SNR}$. The random variables X and Y are exponentially distributed, and Z is chi-square distributed with $2r$ degrees of freedom [22]; the cardinality of the NBI signal vector is r. The PDF of the variables X, Y, and Z are given, respectively, by

$$f_X(x) = (1/2\sigma_x^2)\exp(-x/2\sigma_x^2), x \ge 0, \quad (32)$$

$$f_Y(y) = (1/2\sigma_y^2)\exp(-y/2\sigma_y^2), y \ge 0, \quad (33)$$

$$f_Z(z) = \frac{1}{\sigma_z^{2r}\, 2^r \Gamma(r)} z^{r-1} \exp\left(-z/2\sigma_z^2\right), z \ge 0. \quad (34)$$

Since the desired signal channel and the interference channel are negatively quadrant dependent [23], the outage probability of X for the given random variables Y and Z is given by

$$P_{\text{out},k}^{\text{dir}}(R) \le \int_0^\infty \int_0^\infty P\left(X < \gamma_1 \frac{(by+cz+d)}{a}\Big|_{Y=y,Z=z}\right) f_Y(y) f_Z(z)\,\text{d}y\text{d}z. \quad (35)$$

Since $|v(k,k)| \approx 1$ and $a \approx 1$, (35) can be simplified as

$$P_{\text{out},k}^{\text{dir}}(R) \le \int_0^\infty \int_0^\infty \int_0^{(by+cz+d)\gamma_1} f_X(x) f_Y(y) f_Z(z)\,\text{d}x\text{d}y\text{d}z. \quad (36)$$

Evaluating the inner integral by substituting (32), it becomes

$$P_{\text{out},k}^{\text{dir}}(R) \le \int_0^\infty \int_0^\infty \left[1 - \exp\left(-\gamma_1(by+cz+d)\right)\right] f_Y(y) f_Z(z)\,\text{d}y\text{d}z. \quad (37)$$

Now, (37) can be rewritten as

$$P_{\text{out},k}^{\text{dir}}(R) \le 1 - \text{e}^{-\gamma_1 d} \int_0^\infty \text{e}^{-\gamma_1 by} f_Y(y)\,\text{d}y \int_0^\infty \text{e}^{-\gamma_1 cz} f_Z(z)\,\text{d}z. \quad (38)$$

Substituting (33) and (34) in (38), then integrating, the outage probability is determined as

$$P_{\text{out},k}^{\text{dir}}(R) \le 1 - \exp(-\gamma_1 d)\frac{\left[1 + (\gamma_1 c/r)\right]^{-r}}{(1+\gamma_1 b)}. \quad (39)$$

Substituting b, c, d, and γ_1, the outage probability of the direct-mode SINR in terms of the data rate is given by

$$P_{\text{out},k}^{\text{dir}}(R) \le 1 - \exp\left(-\left(2^R - 1\right)/\text{SNR}\right) \times \frac{\left[1 + \left(\left(2^R - 1\right)\varsigma_3/r\text{SIR1}\right)\right]^{-r}}{\left[1 + \left(2^R - 1\right)\left(1 - |v(k,k)|^2\right)\right]}. \quad (40)$$

2. Outage Probability Analysis in AF Relay Mode

The outage probability for AF relay–mode SINR, Γ_{AF}, at the kth subcarrier is defined as

$$P_{\text{out},k}^{\text{AF}}(R) = P\left((1/2)\log_2\left(1+\Gamma_{\text{AF}}(k)\right) < R\right). \quad (41)$$

Since maximal ratio combining is applied at the destination in the second time slot, the AF relay–mode SINR Γ_{AF} is defined as $\Gamma_{\text{AF}}(k) = \Gamma_{13}(k) + \Gamma_{123}(k)$. Now, (41) can be written as

$$P_{\text{out},k}^{\text{AF}}(R) = P\left(\Gamma_{13}(k) + \Gamma_{123}(k) < 2^{2R} - 1\right). \quad (42)$$

Given the threshold SINR γ_1 for $\Gamma_{13}(k)$, the lower bound of the AF outage probability is given by

$$P_{\text{out},k}^{\text{AF}}(R) \ge \int_0^{2^{2R}-1} P\left(\Gamma_{123}(k) < 2^{2R} - 1 - \gamma_1\right) f_{\Gamma_{13}}(\gamma_1)\,\text{d}\gamma_1. \quad (43)$$

Let $\gamma_2 = 2^{2R} - 1 - \gamma_1$. Then, (43) can be written as

$$P_{\text{out},k}^{\text{AF}}(R) \ge \int_0^{2^{2R}-1} \int_0^{2^{2R}-1-\gamma_1} f_{\Gamma_{123}}(\gamma_2) f_{\Gamma_{13}}(\gamma_1)\,\text{d}\gamma_1\text{d}\gamma_2, \quad (44)$$

where $f_{\Gamma_{123}}(\gamma_2)$ and $f_{\Gamma_{13}}(\gamma_1)$ are PDF functions of $\Gamma_{123}(k)$ and $\Gamma_{13}(k)$, respectively.

Since $\Gamma_{123}(k)$ is the minimum of $\Gamma_{12}(k)$ and $\Gamma_{23}(k)$, the cumulative distribution function (CDF) of $\Gamma_{123}(k)$ can be written as [21]

$$F_{\Gamma_{123}}(\gamma_2) = 1 - \left[\left(1 - F_{\Gamma_{12}}(\gamma_2)\right)\left(1 - F_{\Gamma_{23}}(\gamma_2)\right)\right]. \quad (45)$$

Using (39), the CDF of $\Gamma_{12}(k)$ is computed as

$$F_{\Gamma_{12}}(\gamma_2) = 1 - \exp\left(-\frac{\gamma_2}{\text{SNR}}\right)\frac{\left[1 + \left(\gamma_2\varsigma_2/r\text{SIR2}\right)\right]^{-r}}{(1+\gamma_2 b)}. \quad (46)$$

By using the approximations $\left(1 + (a/r)\right)^{-r} \approx \exp(-a)$ and $|v(k,k)|^2 \approx 1$, (46) can be simplified as

$$F_{\Gamma_{12}}(\gamma_2) = 1 - \exp\left(-\left(1/\text{SNR}\right) - \left(\varsigma_2/\text{SIR2}\right)\right)\gamma_2. \quad (47)$$

Similarly, the CDF of $\Gamma_{23}(k)$ can be expressed as

$$F_{\Gamma_{23}}(\gamma_2) = 1 - \exp\left(-\left(1/\text{SNR}\right) - \left(\varsigma_3''/\text{SIR3}\right)\right)\gamma_2. \quad (48)$$

Substituting (47) and (48) in (45), the CDF of $\Gamma_{123}(k)$ is

obtained as

$$F_{\Gamma_{123}}(\gamma_2) = 1 - \exp\left(-\left(\frac{2}{\text{SNR}} + \frac{\varsigma_2}{\text{SIR2}} + \frac{\varsigma_3''}{\text{SIR3}}\right)\right)\gamma_2 . \quad (49)$$

Let $g_2 = \left(\frac{2}{\text{SNR}} + \frac{\varsigma_2}{\text{SIR2}} + \frac{\varsigma_3''}{\text{SIR3}}\right)$. Then, it can be written as

$$F_{\Gamma_{123}}(\gamma_2) = 1 - \exp(-g_2\gamma_2) . \quad (50)$$

Differentiating (50) with respect to γ_2, the PDF of $\Gamma_{123}(k)$ is determined as

$$f_{\Gamma_{123}}(\gamma_2) = \mathrm{d}\left(F_{\Gamma_{123}}(\gamma_2)\right)/\mathrm{d}\gamma_2 = g_2 \exp(-g_2\gamma_2) . \quad (51)$$

Using (39), the CDF of $\Gamma_{13}(k)$ is given by

$$F_{\Gamma_{13}}(\gamma_1) = 1 - \left[\exp\left(-\frac{\gamma_1}{\text{SNR}}\right)\frac{\left[1+\left(\gamma_1\varsigma_3/\text{SIR1}r\right)\right]^{-r}}{\left[1+\gamma_1\left(1-\left|v(k,k)\right|^2\right)\right]}\right] . \quad (52)$$

It can be simplified as

$$F_{\Gamma_{13}}(\gamma_1) = 1 - \exp(-g_1\gamma_1) , \quad (53)$$

where $g_1 = \left(1/\text{SNR} + \varsigma_3/\text{SIR1}\right)$. Then, the PDF of $\Gamma_{13}(k)$ is determined as

$$f_{\Gamma_{13}}(\gamma_1) = \mathrm{d}\left(F_{\Gamma_{13}}(\gamma_1)\right)/\mathrm{d}\gamma_1 = g_1 \exp(-g_1\gamma_1) . \quad (54)$$

Substituting the PDF of $\Gamma_{123}(k)$ in (44) and evaluating the inner integral, we get

$$P_{\text{out},k}^{\text{AF}}(R) \geq \int_0^{2^{2R}-1}\left[1-\exp\left(-g_2\left(2^{2R}-1-\gamma_1\right)\right)\right] f_{\Gamma_{13}}(\gamma_1)\,\mathrm{d}\gamma_1 . \quad (55)$$

Substituting the PDF of $\Gamma_{13}(k)$ in (55), the lower bound of the outage probability for AF relay mode is determined as

$$P_{\text{out},k}^{\text{AF}}(R) \geq \left[1-\exp\left(-g_1\left(2^{2R}-1\right)\right)\right] - \left[\left(g_1/(g_1-g_2)\right) \times \exp\left(-g_2\left(2^{2R}-1\right)\right)\right]\left[1-\exp\left(-(g_1-g_2)\left(2^{2R}-1\right)\right)\right]. \quad (56)$$

3. Outage Probability for Incremental AF Relaying

In AF relay mode, a relay transmits the amplified received signal at the data rate of R b/s/Hz through a specified channel for the duration of the signal transmission. Indirectly, it reduces the number of degrees of freedom of the channel. But, in incremental AF relaying protocols, data is transmitted at either $R/2$ b/s/Hz or R b/s/Hz. The AF relay transmits data at the rate of $R/2$ b/s/Hz only if the direct-mode transmission fails to send the data at the data rate of R b/s/Hz, thereby an incremental AF relay network utilizes the relay channel effectively and improves the system performance [17]. The outage probability of the incremental AF relay mode is given by

$$P_{\text{out},k}^{\text{IAF}}(R) = P\left(\Gamma_{13}(k) < R\right) \times P\left((1/2)\log_2\left(1+\Gamma_{\text{AF}}(k)\right) < (R/2)\Big|_{\Gamma_{13}(k)<R}\right). \quad (57)$$

In an incremental AF relaying protocol, the intersection of the direct mode and AF relay mode outage probabilities is exactly the AF relay mode outage probability at half the rate of the data rate. Therefore, it can be written as

$$P_{\text{out},k}^{\text{IAF}}(R) = P\left((1/2)\log_2\left(1+\Gamma_{\text{AF}}(k)\right) < (R/2)\right) . \quad (58)$$

Using (56), the lower bound of the outage probability of the incremental AF relay mode is given by

$$P_{\text{out},k}^{\text{IAF}}(R) \geq \left[1-\exp\left(-g_1\left(2^R-1\right)\right)\right] - \left(g_1/(g_1-g_2)\right) \times \exp\left(-g_2\left(2^R-1\right)\right)\left[1-\exp\left(-(g_1-g_2)\left(2^R-1\right)\right)\right]. \quad (59)$$

V. Numerical Results

The outage performance of the proposed OFDM-based CR relay network is analyzed in the presence of an NBI signal for direct, AF relay, and incremental AF relay modes. The simulation parameters are listed in Table 1.

The outage performance of the proposed cognitive AF relay network in direct mode is shown in Fig. 2 for the data rate of 1 b/s/Hz. The SIR is varied from 10 dB to 25 dB. It is observed that the analytical results are very close to the simulation results. As the noise dominates NBI at low SNR, the effect of NBI is more significant at high SNR. In direct mode, as the SIR increases from 20 dB to 25 dB, the outage probability decreases from 1×10^{-2} to 3×10^{-3} at the data rate of 1 b/s/Hz and SNR per subcarrier of 30 dB.

Figure 3 shows the outage performance of the OFDM-based cognitive AF relay network in direct mode for the data rates 1 b/s/Hz and 2 b/s/Hz. It is observed that when the data rate is increased from 1 b/s/Hz to 2 b/s/Hz, the minimum SNR requirement increases from 20 dB to 25 dB in the absence of

Table 1. Simulation parameters of cognitive AF relay network.

S. No	Parameters	Value
1	Number of subcarriers in OFDM signal, N	64
2	Guard sequence length, v	16
3	Number of channel taps, L	10
4	Number of subcarriers with NBI, r	1, 3, 5
5	CFO parameter of NBI signal, β	0.5
6	Data rates (in b/s/Hz), R	0.5, 1, 2, 3
7	Signal to NBI interference ratio (in dB)	10, 15, 20, 25

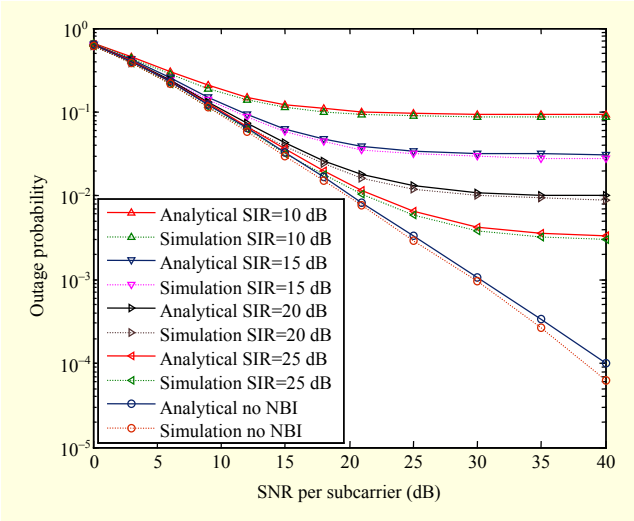

Fig. 2. Outage performance of proposed cognitive AF relay network in direct mode at 1 b/s/Hz.

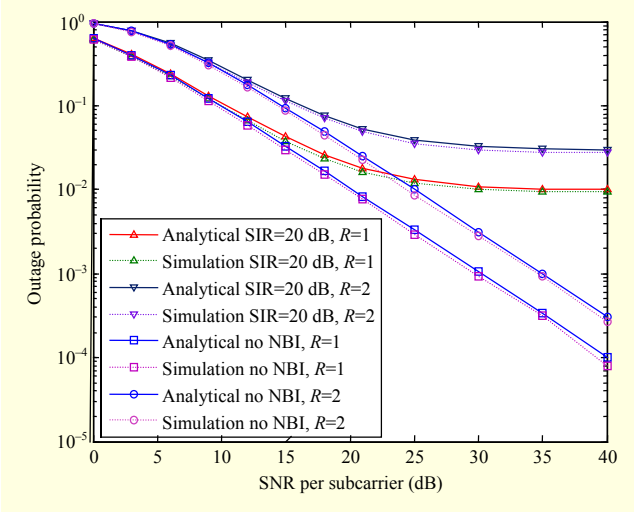

Fig. 3. Outage performance of proposed cognitive AF relay network in direct mode at 1 b/s/Hz and 2 b/s/Hz.

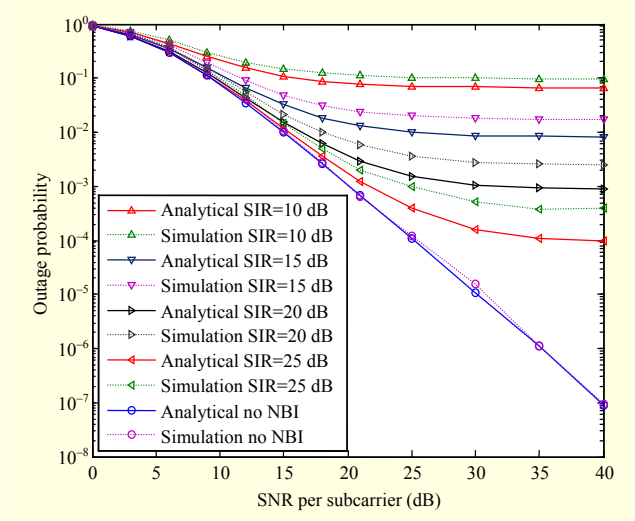

Fig. 4. Outage performance of AF mode transmission at 1 b/s/Hz.

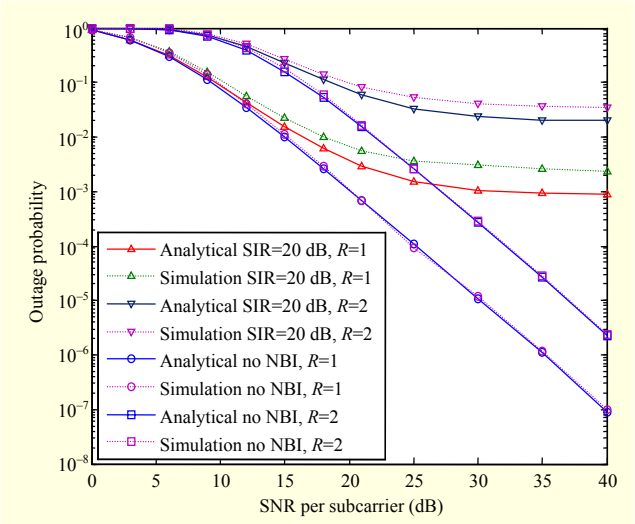

Fig. 5. Outage performance in AF relay mode at 1 b/s/Hz and 2 b/s/Hz.

NBI to operate the network at the maximum outage probability of 1×10^{-2}. The minimum SNR requirement rises to 30 dB SNR with a data rate of 1 b/s/Hz at an SIR of 20 dB.

The outage performance for the proposed OFDM-based CR network in AF relay mode transmission is shown in Fig. 4 at the data rate of 1 b/s/Hz for different SIR values. Since the maximal ratio combining provides diversity gain at the destination node, the minimum SNR requirement decreases to 15 dB from 20 dB in the direct mode transmission at the outage probability of 1×10^{-2}. In AF relay mode at 30 dB SNR, as the SIR increases from 20 dB to 25 dB, the outage probability decreases from 1×10^{-3} to 1×10^{-4} at the data rate of 1 b/s/Hz.

The outage performance of the proposed cognitive network in AF relay mode for the data rates of 1 b/s/Hz and 2 b/s/Hz is shown in Fig. 5. It is observed that when the data rate moves from 1 b/s/Hz to 2 b/s/Hz, the minimum SNR requirement to operate the network at the maximum outage probability of 1×10^{-2} increases from 15 dB to 22 dB in the absence of NBI, and for the SIR level of 20 dB, it further rises to 17 dB SNR with a data rate of 1 b/s/Hz and exceeds the limit at a data rate of 2 b/s/Hz.

The outage performance at the direct and AF relay modes is compared in Fig. 6. It is observed that the AF mode provides 5 dB SNR gain compared to the direct mode in the absence of NBI. At 30 dB SNR, when the mode is switched from direct to AF relay, the outage probability decreases from 1×10^{-2} to 1×10^{-3} at a data rate of 1 bit/s/Hz with 20 dB SIR.

In Fig. 7, the outage performance of the proposed OFDM-

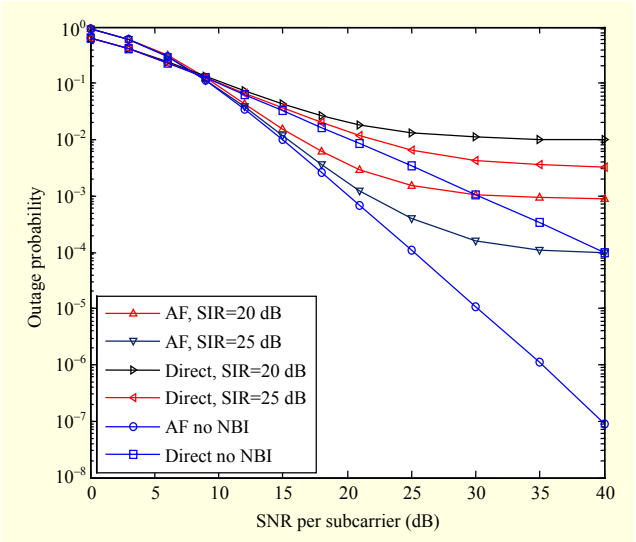

Fig. 6. Comparison of outage performance in AF relay mode and direct mode at 1 b/s/Hz.

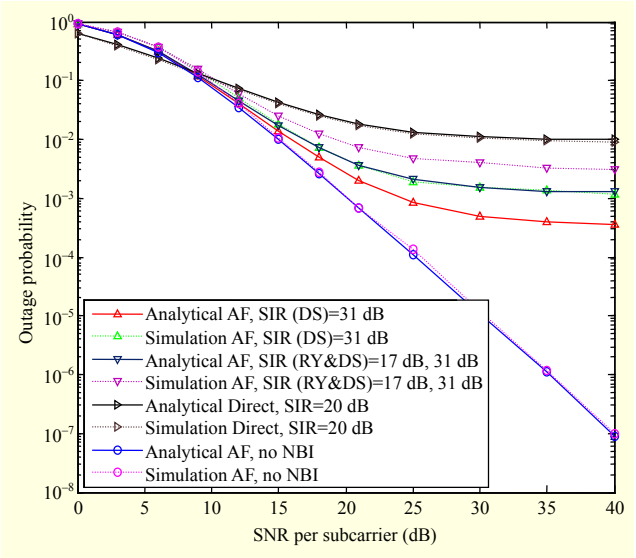

Fig. 7. Comparison of outage performance in AF relay and direct modes at 1 b/s/Hz, with and without NBI at relay.

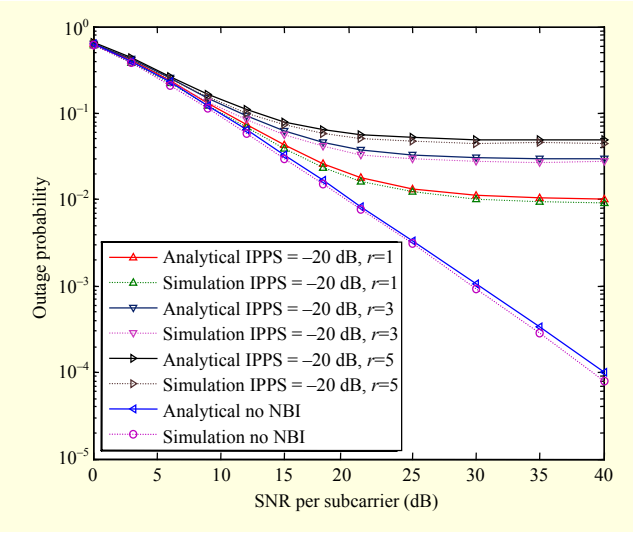

Fig. 8. Outage performance of proposed cognitive AF relay network in direct mode at 1 b/s/Hz for various r values.

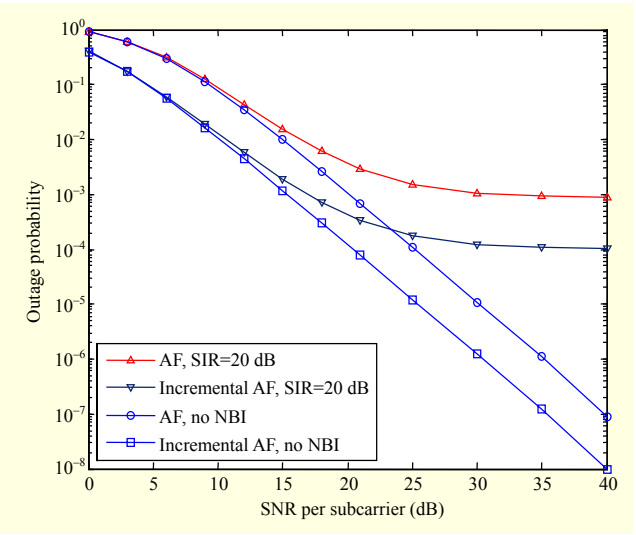

Fig. 9. Comparison of outage performance in AF relay and incremental AF relay modes at 1 b/s/Hz.

based CR network in AF relay mode is compared with direct mode for various relay interference values. The data rate is 1 b/s/Hz. In this Figure, RY and DS denote the relay and destination nodes, respectively. It is noted that the outage probability decreases from 1×10^{-3} to 4×10^{-4} when relay node operates with no NBI, at 30 dB SNR per subcarrier. In direct mode, the outage probability of the network is 1×10^{-2} for an SIR of 20 dB and an SNR of 30 dB. It indicates that the proposed network with limited interference at the relay performs better than the direct mode.

In Fig. 8, r represents the number of subcarriers that are directly affected by NBI. The outage performance of the proposed CR network in direct mode is shown in Fig. 8 at a data rate of 1 b/s/Hz for different r values. At 30 dB SNR, when r decreases from five to three, the outage probability decreases from 4.4×10^{-2} to 2.7×10^{-2}; furthermore, it reduces to 1×10^{-2} when $r = 1$.

The outage performance of the AF relay and incremental AF relay modes is compared in Fig. 9. It is observed that for the outage probability of 1×10^{-4}, the incremental AF relay mode provides 5 dB SNR gain compared to the AF relay mode, in the absence of NBI. This is due to the additional degree of freedom in the incremental AF relay mode.

The outage performance of the AF relay mode for the data

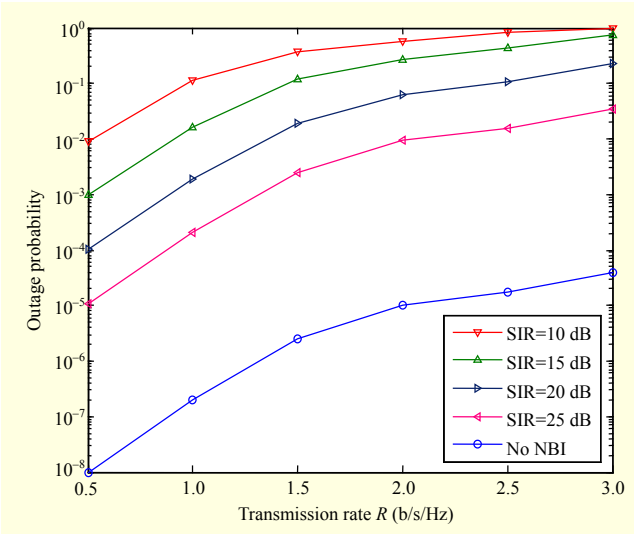

Fig. 10. Outage performance of AF relay mode vs. transmission rates for fixed SNR = 40 dB.

rates between 0.5 b/s/Hz and 3 b/s/Hz is shown in Fig. 10. At a low data rate, the outage is exactly reduced by 1×10^{-1} for every 5 dB increase in SIR level. For the maximum outage probability of 1×10^{-2}, the CR network supports a data rate of up to 2 b/s/Hz at 25 dB SIR.

VI. Conclusion

In this paper, a fixed AF relaying protocol is introduced in an OFDM-based CR network to suppress the effect of NBI. The performance of the CR network with an AF relay is analyzed in terms of outage probability. It is shown that the use of the AF relay suppresses the effect of NBI and that the outage performance is improved by 5 dB per subcarrier compared to the direct-mode transmission at a data rate of 1 b/s/Hz. Further, the outage performance is improved by the incremental AF relaying, where the system is operated at variable rate nature. It is found that for no NBI at the relay node, the outage of the system is significantly reduced. Finally, we conclude that the effect of the NBI can be reduced by the AF relay protocol in an OFDM-based cognitive radio system at constant data rate.

References

[1] S. Haykin, "Cognitive Radio: Brain-Empowered Wireless Communications," *IEEE J. Sel. Areas Commun.*, vol. 23, no. 2, Feb. 2005, pp. 201–220.

[2] H.A. Mahmoud, T. Yücek, and H. Arslan, "OFDM for Cognitive Radio: Merits and Challenges," *IEEE Wireless Commun.*, vol. 16, no. 2, Apr. 2009, pp. 6–15.

[3] X. Hong et al., "Cognitive Radio Networks: Interference Cancellation and Management Techniques," *IEEE Veh. Technol. Mag.*, vol. 4, no. 4, Dec. 2009, pp. 76–84.

[4] A. Batra and J.R. Zeidler, "Narrowband Interference Mitigation in OFDM Systems," *IEEE Military Commun. Conf.*, San Diego, CA, USA, Nov. 16–19, 2008, pp. 1–7.

[5] A.J. Coulson, "Bit Error Rate Performance of OFDM in Narrowband Interference with Excision Filtering," *IEEE Trans. Wireless Commun.*, vol. 5, no. 9, Sept. 2006, pp. 2484–2492.

[6] H. Yamaguchi, "Active Interference Cancellation Technique for MB-OFDM Cognitive Radio," *IEEE European Microw. Conf.*, Amsterdam, Netherlands, Oct. 12–14, 2004, pp. 1105–1108.

[7] C.W. Baum and M.B. Pursley, "Bayesian Methods for Erasure Insertion in Frequency-Hop Communication Systems with Partial Band Interference," *IEEE Trans. Commun.*, vol. 40, no. 7, July 1992, pp. 1231–1238.

[8] A.J. Redfern, "Receiver Window Design for Multicarrier Communication Systems," *IEEE J. Sel. Areas Commun.*, vol. 20, no. 5, June 2002, pp. 1029–1036.

[9] R. Nilsson, F. Sjoberg, and J. LeBlanc, "A Rank-Reduced LMMSE Canceller for Narrowband Interference Suppression in OFDM-Based Systems," *IEEE Trans. Commun.*, vol. 51, no. 12, Dec. 2003, pp. 2126–2140.

[10] L. Sanguinetti, M. Morelli, and H.V. Poor, "Robust EM-Based Detection of BICM-OFDM Transmissions in the Presence of Narrowband Interference," *IEEE European Wireless Conf.*, Lucca, Italy, Apr. 12–15, 2010, pp. 696–700.

[11] D. Darsena et al., "A Constrained Maximum-SINR NBI-Resistant Receiver for OFDM Systems," *IEEE Trans. Signal Process.*, vol. 55, no. 6, June 2007, pp. 3032–3047.

[12] A. Gomaa and N. Al-Dhahir, "A Sparsity-Aware Approach for NBI Estimation in MIMO-OFDM," *IEEE Trans. Wireless Commun.*, vol. 10, no. 6, June 2011, pp. 1854–1862.

[13] K. Maichalernnukul, T. Kaiser, and F. Zheng, "Performance of Ultra-wideband Cooperative Relay Systems in the presence of Narrowband Interference," *IEEE Int. Conf. Ultra-wideband*, Bologna, Italy, Sept. 14–16, 2011, pp. 405–409.

[14] M.H. Hassan and Md. J. Hossain, "Cooperative Beamforming for Cognitive Radio Systems with Asynchronous Interference to Primary User," *IEEE Trans. Wireless Commun.*, vol. 12, no. 11, Nov. 2013, pp. 5468–5479.

[15] P. Popovski et al., "Opportunistic Interference Cancellation in Cognitive Radio Systems," *IEEE Dynamic Spectr. Access Netw.*, Dublin, Ireland, Apr. 17–20, 2007, pp. 472–475.

[16] E.H.M. Alian and P. Mitran, "A Phase Adjustment Approach for Interference Reduction in OFDM-Based Cognitive Radios," *IEEE Trans. Wireless Commun.*, vol. 12, no. 9, Sept. 2013, pp. 4668–4679.

[17] J.N. Laneman, D.N.C. Tse, and G.W. Wornell, "Cooperative Diversity in Wireless Networks: Efficient Protocols and Outage Behavior," *IEEE Trans. Inf. Theory*, vol. 50, no. 12, Dec. 2004, pp. 3062–3080.

[18] B. Muquet et al., "Cyclic Prefixing or Zero Padding for Wireless Multicarrier Transmissions?" *IEEE Trans. Commun.*, vol. 50, no. 12, Dec. 2002, pp. 2136–2148.
[19] A. Batra and J.R. Zeidler, "Narrowband Interference Mitigation in BICM OFDM Systems," *IEEE Acoust. Speech Signal Process.*, Taipei, Taiwan, Apr. 19–24, 2009, pp. 2605–2608.
[20] R.M. Gray, *Toeplitz and Circulant Matrices: A Review*, Hanover, MA, USA: Now Publishers Inc., 2006, pp. 155–239.
[21] P. Rabiei, W. Namgoong, and N. Al-Dhahir, "On the Performance of OFDM-Based Amplify-and-Forward Relay Networks in the Presence of Phase Noise," *IEEE Trans. Commun.*, vol. 59, no. 5, May 2011, pp. 1458–1466.
[22] J.G. Proakis and M. Salehi, "*Digital Communication*," New York, USA: Mc-Graw Hill, 2008, pp. 1–1150.
[23] E.L. Lehmann, "Some Concepts of Dependence," *Ann. Mathematical Statistics*, vol. 37, no. 5, 1966, pp. 1137–1153.

Samikkannu Rajkumar received his BE degree in electronics and communication engineering from the Angala Amman College of Engineering and Technology, Tamil Nadu, India, in 2000 and his ME degree in communication systems from Thiagarajar College of Engineering, Tamil Nadu, India, in 2006. At present, he is working as a full-time research scholar with the Department of Electronics and Communication Engineering, Thiagarajar College of Engineering, Tamil Nadu, India. His current areas of research include developing algorithms in cooperative relay networks and multiple antenna systems.

V.N. Senthilkumaran received his BE degree in electronics and communication engineering from VelTech Engineering College, Tamil Nadu, India, in 2002. He obtained his ME degree in communication systems from S.R.M. Engineering College, Tamil Nadu, India, in 2004 and his PhD degree in the area of wireless relay network design from Anna University, Tamil Nadu, India, in 2014. At present, he is working as an assistant professor with the Department of Electronics and Communication Engineering, Thiagarajar College of Engineering, Tamil Nadu, India. His current areas of research include physical-layer network coding and capacity analysis of wireless networks.

S.J. Thiruvengadam received his BE degree in electronics and communication engineering from Thiagarajar College of Engineering, Tamil Nadu, India, in 1991. He obtained his ME degree in applied electronics from the College of Engineering, Tamil Nadu, India, in 1994 and his PhD degree in the area of signal detection algorithms from Madurai Kamaraj University, Tamil Nadu, India, in 2005. At present, he is working as a professor with the Department of Electronics and Communication Engineering, Thiagarajar College of Engineering. Previously, he was a visiting associate professor with the Department of Electrical Engineering, Stanford University, CA, USA, under a postdoctoral fellowship sponsored by the Department of Science and Technology, Government of India, from January to December 2008. His current areas of research include statistical signal processing and multiple-input and multiple-output wireless communications.